Supplementary Online Material

Supplementary Data

Calibration curve

To confirm adequate solubilization of the dried spotted RNA probes and to exclude the possibility that a large fraction of the solvents stick to the polydimethylsiloxane (PDMS) composing the microfluidic device, we generated a calibration curve. Known concentrations of soluble labeled RNA probes were loaded into the device by continuous flow and mean values of Cy3 signal from multiple unit cells were averaged. Based on this curve, we calculated the actual concentration of target RNA sequences used in our assay. On average the actual assayed concentration was 0.55±0.02 of the spotted one. Of note, a similar factor (0.57) was calculated based on the ratio between a typical print volume and unit cell volume. All the presented data were adjusted according to this factor.

RNA binding experiment with high ionic strength buffer

The ionic strength of the buffer used in an RNA binding experiment may have an effect on the protein-RNA interaction. To confirm that the high affinity interactions detected in our RNA binding assay are not a result of enhancement of electrostatic interactions due to a low ionic strength buffer we performed RNA binding experiments of NS4B by microfluidics using high (150mM) ionic strength conditions. RNA binding by NS4B in the presence of PBS (137 mM NaCl, 2.7 mM KCl, 10 mM Na_2HPO_4, 2 mM KH_2PO_4) or 150mM Hepes was similar to that detected with 50mM Hepes buffer, commonly used for RNA binding assays by others ([1], [2]). The Kd of NS4B binding to the 3' terminus of the HCV negative strand RNA in the high ionic strength conditions was measured at 6.6±3.3 nM (vs. a Kd of 3.4±1.0 nM in the presence of low (50mM) ionic strength conditions). These results suggest that there is only a small electrostatic component to the observed RNA-binding.

ATA inhibits RNA binding by NS4B in a dose-dependent manner

Prior to the library screen we wished to determine whether HCV RNA binding by NS4B can be inhibited pharmacologically. Aurintricarboxilic acid (ATA) is a compound known to inhibit interactions of proteins with nucleic acids [3]. We thus hypothesized that ATA may similarly inhibit binding of NS4B to HCV RNA. To test this hypothesis, the NS4B RNA binding assay was repeated in the presence of increasing concentrations of ATA. Indeed, ATA was found to inhibit binding of HCV RNA by NS4B in a dose-dependent manner, with an IC 50 of 0.49±0.01μM (p value – 0.0003) (fig. 5S).
To our surprise, having not previously realized that ATA was one of the compounds included in the LOPAC library, ATA was one of the 18 compounds identified in the screen. Since we had previously shown that this compound inhibits the RNA binding activity of NS4B, this turned to be a useful internal control for the validity of our screen.

Specificity of hits identified in the small molecule screen

To determine the specificity of the hits identified in our small molecule screen we chose the HuR protein (one of the human RNA binding protein used to validate our RNA binding assay). Interestingly, other than binding to its target RNA sequence, 4A (fig. 3S),

this protein has been previously shown by others [4] to bind the 3' terminus of the negative HCV strand. Binding of HuR to the consensus 4A RNA sequence was tested in the presence of the inhibitory molecules shown to inhibit RNA binding by NS4B. No inhibitory effect on RNA binding was detected with the majority of the hits including clemizole at a concentration of 0.1mM. Similarly, 0.1mM of the identified compounds didn't have an inhibitory effect on binding of HuR to the 3' terminus of the negative HCV RNA strand. In contrast to the other hits, ATA, known as a non-specific inhibitor of protein-nucleic acids interactions, significantly inhibited HuR binding to both 4A and 3' terminus of the negative HCV strand. These results suggest that the identified hits including clemizole are indeed specific to RNA binding by NS4B.

Supplementary figures

Supplementary Figure 1

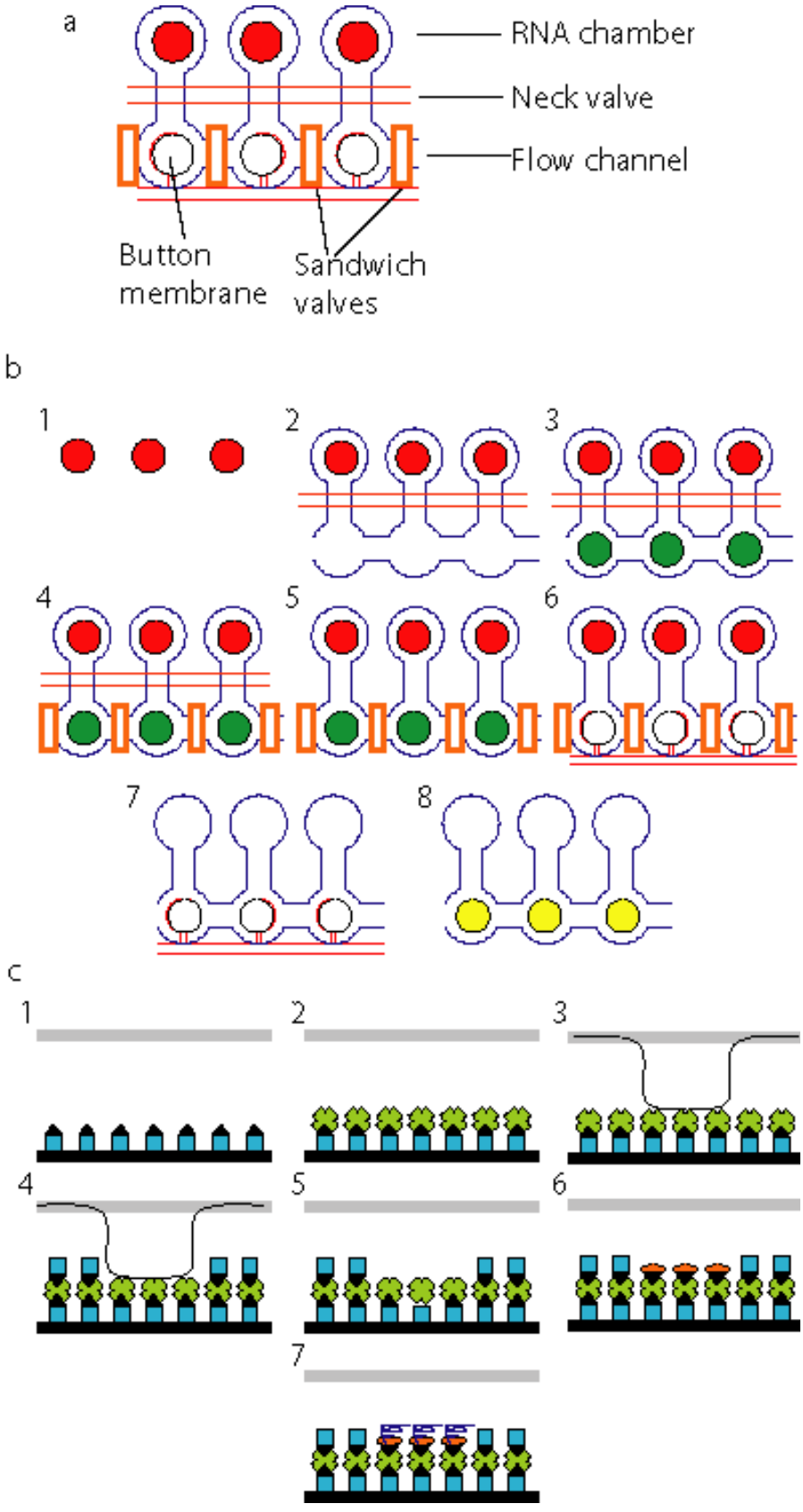

Microfluidic based RNA binding assay. 3 individual unit cells (out of hundreds/thousands per microfluidic device) are shown in this scheme.

a- Compartments and micromechanical valves. A valve is created where a control channel crosses a flow channel. The resulting thin membrane in the junction between the two channels can be deflected by hydraulic actuation.Using multiplexed valve systems allows a large number of elastomeric microvalves to perform complex fluidic manipulations within these devices.

b- Experimental protocol. ● represents Cy3 labeled RNA probe. ● represents surface bound bodipy-labeled protein. 1) target RNA sequences labeled with Cy3 were spotted onto an epoxy-coated slide as a microarray 2) The microfluidic device was aligned and bonded to the slide allowing contact of each spot in the array with a unit cell in the device. The device was subjected to surface patterning that resulted in a circular area coated with biotinylated anti-histidine antibodies within each unit cell (see c). The "neck valve" separating the flow channels from the RNA chamber remained closed during this process. 3) The device was then loaded with *in vitro* transcription/ translation mixture containing DNA template encoding a his-labeled protein. Bodipy-labeled tRNALys was added for protein labeling. 4) Each unit cell was then isolated by the control of two "sandwich" micromechanical valves. 5) the "neck valve" was opened forming a single compartment by combining the flow channel compartment with the RNA chamber. This was followed by an incubation to allow protein synthesis, binding of the synthesized protein to the surface biotinylated anti-his antibodies, solvation of target RNA, and equilibration of proteins and target RNA. 6) MITOMI was then performed by actuation of a "button" membrane trapping surface-bound complexes while expelling any solution phase molecules. 7) The "sandwich" valves were opened followed by a brief wash to remove untrapped unbound material. 8) the "button" membrane was opened and the device was scanned by an array scanner. Trapped RNA molecules and expressed protein were detected. The ratio of bound RNA to expressed protein was calculated for each data point by measuring the median signal of Cy3 to median signal of bodipy (represented by ●).

c- Surface patterning. 1)Accessible surface area was derivatized by flowing a solution of biotinylated BSA ( ) through all flow channels 2) a Neutravidin solution ( ) was loaded 3) The "button" membrane was activated 4) all remaining accessible surface area except for a circular area of 60 µm masked by the button was passivated with biotinylated solution ( ) 5) the "button" membrane was opened 6)a solution of biotinylated-antibody ( ) was loaded allowing specific functionalization of the previously masked circular area 7) *In vitro* expressed protein ( ) was loaded into the device and bound to the biotinylated-antibody coating the discrete circular area. Each of the described steps was followed by a PBS wash.

Supplementary Figure 2

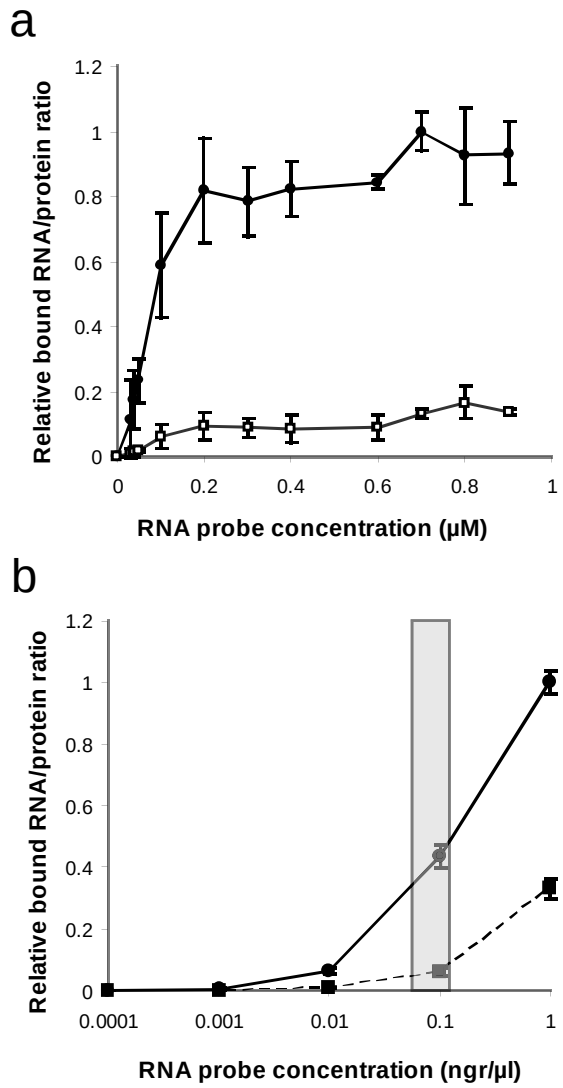

Signal to noise ratio in our RNA binding assay.

a- Binding of HuD-his (●) and Gus-his (□) to increasing concentration of the AU3 RNA probe.

b- Binding of NS4B-GFP-microsomal membranes (mm) (●, continuous line) and NS5A(AH)-GFP-mm (■, dashed line) to increasing concentrations of the 3' terminus of the negative strand.
The grey striped column represents the range of probe concentration for which the signal to noise ratio was the greatest. All of our reported experiments were performed within this range.

Representative experiments are shown. Bars represent standard deviation.

Supplementary Fig. 3

a

		RNA probe sequence	Phenotype (by mobility shift assay/UV cross linking)
4A	$(AUUU)_4A$	AUUUAUUUAUUU AUUUA	Binding
2A	$(AUUU)_2A$	AUUUAUUUA	No binding
4C	$(CUUU)_4C$	CUUUCUUUCUUU CUUUC	No binding

b

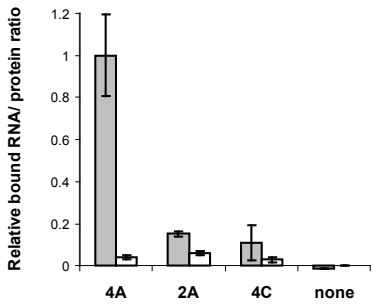

C

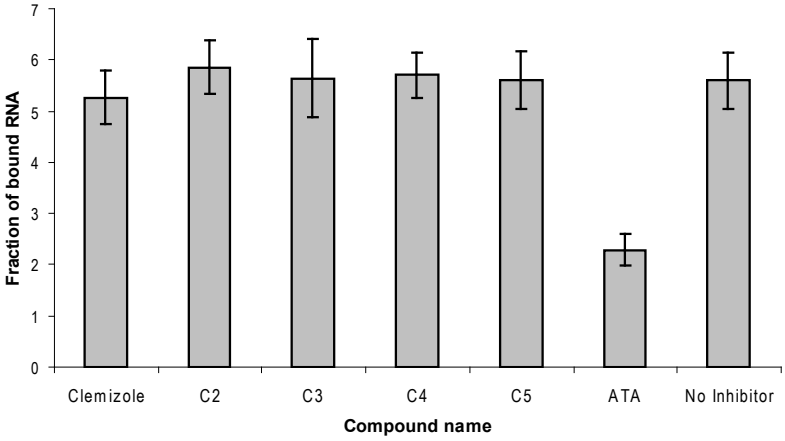

Microfluidics-based analysis of RNA binding by another human protein from the ELAV-like family, HuR (ELAV L1).

a. Target RNA sequences used to study binding of HuR to RNA and the phenotype demonstrated by conventional RNA binding methods 5.

b. HuR binds RNA by microfluidics. A microarray of Cy3-labeled target RNA sequences was used to program a microfluidic device, and binding of bodiby-labeled proteins expressed on the device to the RNA sequences was assayed. Results represent the ratio of bound RNA (median Cy3 signal) to expressed protein (median bodipy signal). Normalized mean values for 10-20 replicates measured in two independent experiments are shown. Error bars represent standard deviation. The grey bars represent binding of HuR-his and the clear bars that of Gus-his, used as a negative control.

c. HUR RNA binding is not affected by the 5 most active compounds, but is affected by ATA. We tested binding of HUR to its 4A RNA target in the presence and absence of NS4B RNA binding inhibitors. Data represent mean value of 10-20 replicates and bars represent standard deviation.

Supplementary Figure 4

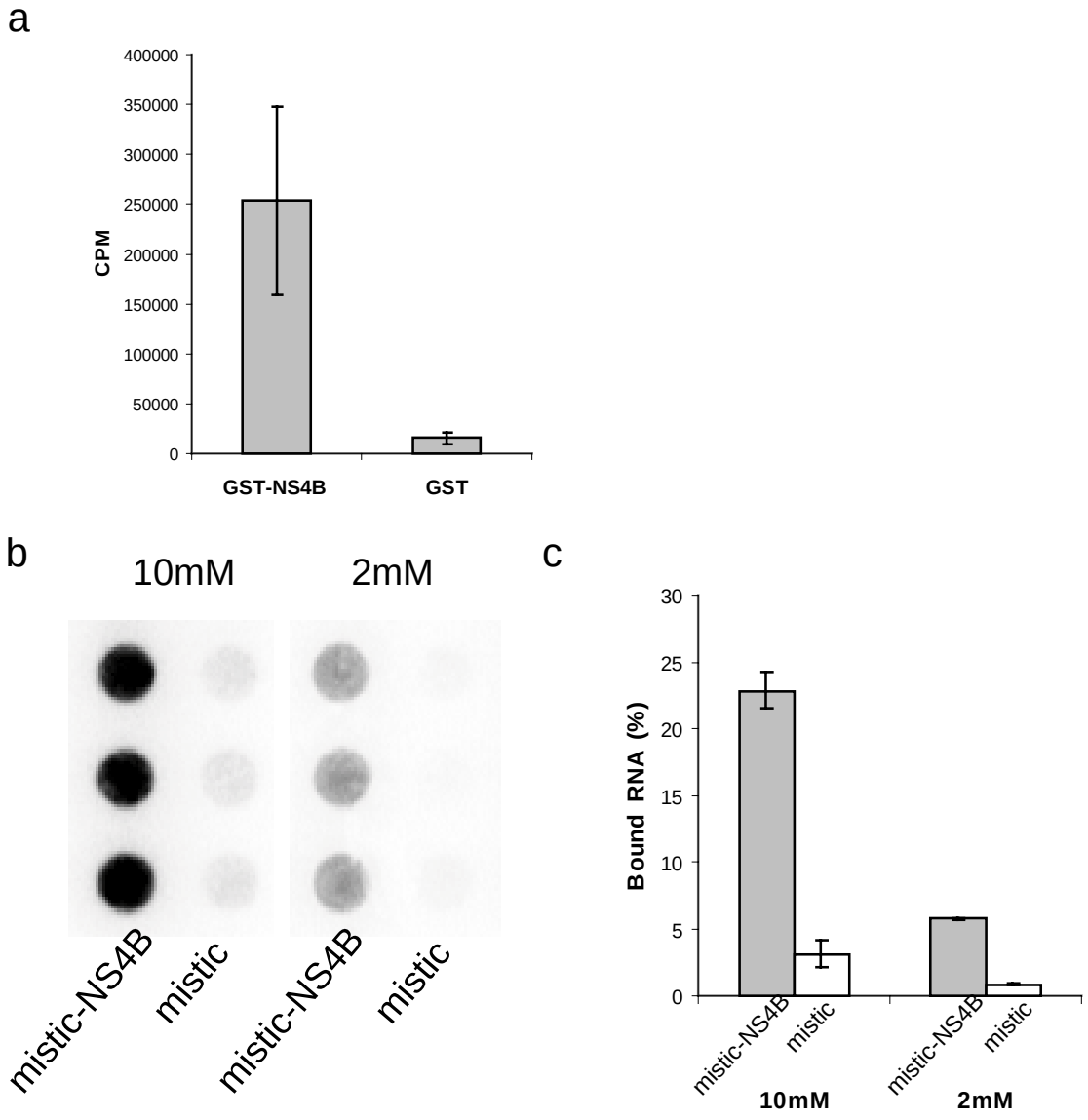

Binding of NS4B to HCV RNA by conventional methods. NS4B was expressed in E.coli fused to GST or mistic-6his and purified. a. Binding activity of GST-NS4B and GST to ^{32}P-labeled RNA probe corresponding to the 3' terminus of the negative viral strand, as measured by a GST pull down assay. b. Nitrocellulose membranes from a representative RNA filter binding assay. ^{32}P-labeled HCV RNA probe bound to 10mM (left panel) or 2mM (right panel) mistic-NS4B or mistic control is shown. c. Percentage of bound RNA to mistic-NS4B and mistic proteins at protein concentrations of 10mM (grey bars) and 2mM (white bars), as measured by a filter binding assay.

Supplementary Figure 5

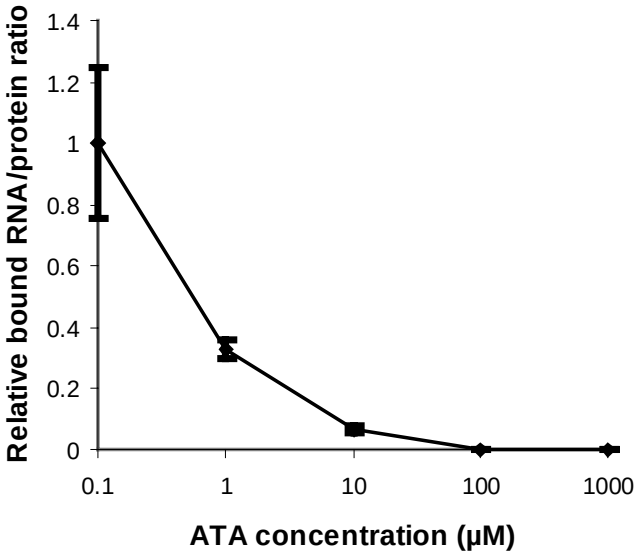

ATA inhibits RNA binding by NS4B in a dose dependent manner. A dose response curve of RNA binding by NS4B in the presence of increasing concentrations of ATA, as measured by microfluidics. The Y category is bound RNA to protein ratio relative to binding in the absence of ATA. The X category is ATA concentration (µM). Data were fit to a 3 parameter logistic curve using the formula Y=a+(b-a)/(1+10^(X-c)) (BioDataFit, Chang Bioscience) and IC50 was calculated at 0.49±0.01 µM (p value - 0.0003).

Supplementary Figure 6

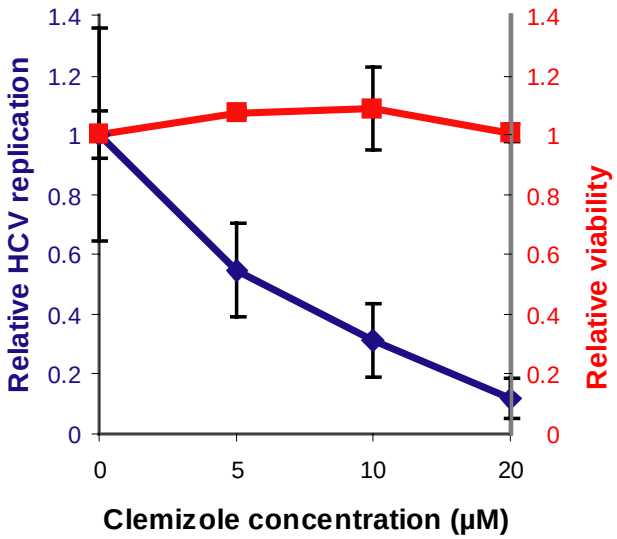

Clemizole inhibits HCV replication by real-time PCR assays. Real-time PCR assay in HCV infected cells showing that clemizole inhibits HCV replication (left axis, blue ♦) with no measurable toxicity to the cell (right axis, red ■).

Supplementary References

1. Huang, L. et al. Hepatitis C virus nonstructural protein 5A (NS5A) is an RNA-binding protein. *J Biol Chem* **280**, 36417-36428 (2005).
2. Nayak, A. et al. Role of RNA structure and RNA binding activity of foot-and-mouth disease virus 3C protein in VPg uridylylation and virus replication. *J Virol* **80**, 9865-9875 (2006).
3. Hallick, R.B., Chelm, B.K., Gray, P.W. & Orozco, E.M. Use of aurintricarboxylic acid as an inhibitor of nucleases during nucleic acid isolation. *Nucleic acids res* **4**, 3055-3064 (1977).
4. Spångberg, K., Wiklund, L. & Schwartz, S. HuR, a protein implicated in oncogene and growth factor mRNA decay, binds to the 3' ends of hepatitis C virus RNA of both polarities. *Virology* **274**, 378-390 (2000).
5. Myer, V.E., Fan, X.C. & Steitz, J.A. Identification of HuR as a protein implicated in AUUUA-mediated mRNA decay. *EMBO J* **16**, 2130-2139 (1997).